



Ethylene epoxidation over shape-selective silver-based catalysts

Kaveh Shariati, Azadeh Mehrani, Trevor Corsello, Mason Kelley, Jochen Lauterbach ^{*}

Department of Chemical Engineering, University of South Carolina, Columbia, SC 29208, United States



ARTICLE INFO

Keywords:

Silver nanowires
Modified polyol method
Ethylene epoxidation
Cesium promotion

ABSTRACT

The catalytic activity and selectivity of silver catalysts in the ethylene epoxidation reaction are intrinsically linked to their faceting. Here, silver nanowires, representing Ag(100), and silver spherical catalysts, embodying Ag(111), were synthesized using modified polyol and wet impregnation methods, respectively. Recognizing the size-dependent nature of catalysis, two distinct sizes of spherical particles were synthesized to serve as comparative benchmarks for silver nanowire activity and selectivity. Silver spherical catalysts were promoted with optimal cesium loading. Furthermore, silver nanowires underwent cesium promotion at varying loadings, as meticulously detailed in the methodology. Unpromoted silver nanowires exhibited superior ethylene oxide selectivity compared to both unpromoted and promoted spherical catalysts. Additionally, the ethylene oxide selectivity was enhanced with the addition of the promoter, achieving activity and selectivity levels comparable to the best reported in the literature. Morphological analysis of spent silver nanowire catalysts revealed exceptional stability even after extended study periods.

1. Introduction

Ethylene oxide (EO) stands as a prominent product within the petrochemical industry, constituting approximately half of the aggregate production of organic chemicals through heterogeneous catalytic oxidation [1–3]. EO boasts diverse applications, ranging from direct utilization as a sterilizer and disinfectant to serving as a critical intermediate for the synthesis of other valuable compounds, such as ethylene glycol. Consequently, EO finds application in a broad spectrum of industries, contributing to the formulation of antifreeze, detergents, as well as serving as a fundamental building block for polyester and polyurethane production [2].

The expansive utility of EO has translated into a robust market presence, with a recorded value of 52.62 billion US dollars in 2021. Projections indicate a continued upward trajectory, anticipating a market value of 75.35 billion USD by 2029, reflective of a growth rate of 4.59 % [4]. Given the substantial economic implications of the EO market, efforts to enhance the selectivity of EO synthesis remain a focal point of research. Significantly, this dedication endures, even in light of the initiation of the ethylene epoxidation reaction by Lefort in 1931 [5], emphasizing the enduring importance of progressing the field.

Fig. 1 illustrates the general ethylene epoxidation reaction (EPO) pathways for the formation of EO and other undesired by-products using silver-based catalysts. Surface science studies have elucidated the

presence of the Oxametallacycle (OMC) intermediate, which subsequently undergoes isomerization to form either EO or acetaldehyde (AA) [6]. Acetaldehyde serves as an intermediate, rapidly generating CO₂ and water. Given the highly exothermic nature of CO₂ formation, the ethylene conversion is intentionally maintained at a low level (7–15 %) [3] to achieve heightened EO selectivity and to regulate the heat generated by the overall combustion pathway [6]. The reaction is conducted at temperatures and pressures ranging from 220 to 275 °C and 1–2.2 MPa, respectively [2,3]. Silver is employed as the exclusive catalyst, supported by alpha aluminum oxide, which plays a crucial role in catalyst stability. As the most stable phase of alumina, α -alumina has the lowest concentration of hydroxyl (OH) groups, minimizing side reactions [1]. Industrial silver particle sizes typically range from 100 nm to 1000 nm [1,3]. Exclusivity of the silver catalysts demonstrating feasible selectivity in the partial oxidation of ethylene to EO ethylene oxide (EO), distinguishing it from common oxidation catalysts like Pd, Pt, or Ni [7], which induce complete combustion. Comparative studies with other transition metals such as Au and Cu [6,8,9] reveal that while all three metals exhibit surfaces with varying selectivities, Ag surfaces consistently demonstrate higher EO selectivity. The optimal selectivity relies on a delicate balance in the metal-oxygen interaction strength, ensuring sufficient dissociation of O₂ for stable atomic oxygen species essential for epoxidation while avoiding excessive binding that could hinder desorption or induce unwanted side reactions. The weakly bound

* Corresponding author.

E-mail address: lautera@cec.sc.edu (J. Lauterbach).

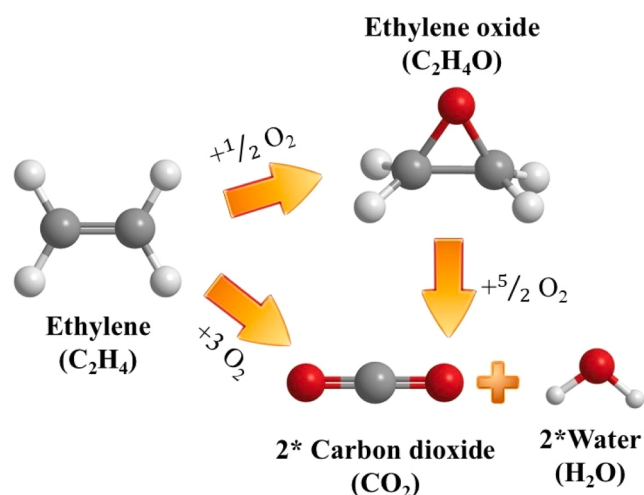


Fig. 1. General schematic of ethylene epoxidation reaction.

oxygens on the silver surface prove advantageous, activating the $C=C$ double bond rather than C–H bonds, and enhancing EO formation. This distinctive feature arises from the moderate activation barriers and binding of the species facilitated by the silver surface [9,10]. In the absence of any promoter, the ethylene and oxygen mixture over the Ag/ α -Al₂O₃ catalyst yields ethylene oxide with approximately 50 % selectivity [11]. Notably, the introduction of promoters such as Cs, Re, and Mo, along with volatile chlorine-containing compounds such as ethyl chloride as a feed additive, results in a remarkable increase in selectivity [3,12].

Despite the necessity of promoters for achieving optimal EO performance in supported Ag/ α -Al₂O₃ catalysts, limited knowledge exists regarding the state and distribution of these promoters. They may be dispersed on both the Ag nanoparticles and the α -Al₂O₃ support, favoring one over the other, or combined in various configurations [13]. The electric field induced by alkali metals, as demonstrated computationally, affects charge transfer, making the formation of EO more favorable than AA formation, thereby stabilizing the transition state for EO [14,15]. Furthermore, computational calculations have revealed that alkali metals lower the activation barrier for O₂ dissociation [14], a fact supported by experimental evidence. Kinetic studies suggest that the promotion effect stems from the reduction in the activation barrier for the dissociative adsorption of molecular O₂ [16,17]. In general, the impact of Cs on electronic effects can be outlined as follows: 1. The polarizable Cs⁺ stabilizes transition states for the EO formation, potentially through the induction of an electric field. 2. It affects the energy barrier for both ethylene oxide and acetaldehyde formation, with a more pronounced effect on acetaldehyde formation, leading to a substantial separation in ΔE_A between the two products. 3. Cs facilitates oxygen dissociation, as the rate-determining step [13].

There is extensive research on various promoters [6,18,19] and secondary metals [8] to improve EO selectivity; however, the EPO reaction still attracts significant attention for further investigation due to EO's high market value. More importantly, the relationship between selectivity, activity, and the facets of the catalyst has received comparatively less exploration experimentally. This aspect has not been extensively exploited in industrial applications, primarily attributed to challenges associated with the preparation and durability of less stable silver surfaces [20]. Computational studies have predominantly addressed the impact of silver faceting on the activity and EO selectivity of the reaction [20,21]. Notably, Hus et al [20] demonstrated that Ag (100) exhibits the highest selectivity among various silver facets, with the lowest apparent activation energy for EO formation, resulting in elevated EO selectivity ranging from 70 % to 80 %. In contrast, Ag(111), characterized by the highest thermodynamic stability, displayed a

moderate EO selectivity (~50 %) [20], as discussed previously. Experimental investigations revealed that silver nanowires and nanocubes predominantly feature Ag(100), while silver spherical particles are primarily composed of Ag(111) [22,23]. However, to the best of the authors' knowledge, few experimental studies [22,24] have systematically explored the impact of silver faceting on the activity and selectivity in ethylene epoxidation reactions. A study by Christopher et al [22] corroborated computational findings, demonstrating that silver nanowires and nanocubes exhibit higher EO selectivity at comparable ethylene conversion levels compared to silver spherical particles [22]. However, numerous unanswered questions persist, highlighting the need for further studies to reveal deeper insights.

There are various synthesis methods for silver nanowires [25]. The modified polyol method stands out as one of the most popular due to its cost-effectiveness, mild reaction conditions, and suitability for industrial production [26]. Additionally, our previous work [27] demonstrated that alternative methods, such as the hydrothermal method, are impractical for EPO reaction applications. This is attributed to the use of glucose, which carbonizes to graphite, and a much thinner diameter that tends to sinter sooner [28]. In the modified polyol method, the controlling agent plays a pivotal role in regulating the growth rate of the nanowires, as opposed to the vigorous stirring required in the polyol method [22,29,30]. Typically, Cl salt serves as the controlling agent. Among numerous polyols, ethylene glycol is widely accepted, serving as both a reducing agent and a solvent [31]. Silver ions (Ag⁺) are supplied by a silver precursor, and ethylene glycol reduces these ions to Ag⁰, which is necessary to form silver seeds. The combination of these silver seeds results in decahedral shapes known as multi-twinned particles (MTPs). Subsequently, Ag⁰ can either join existing MTPs to form nanowires or create new MTPs [28,31]. Therefore, controlling the release rate of Ag⁰ is crucial; otherwise, the aggregation of additional Ag⁰ or MTPs may lead to the formation of larger particles through the Ostwald Ripening process [30]. The presence of Cl⁻ is essential as it reacts with silver ions to form AgCl, which exhibits low solubility in ethylene glycol. Consequently, AgCl is slowly reduced, ensuring a controlled release rate of Ag⁰. The MTPs possess both (111) and (100) facets [30]. The anisotropic growth of MTPs occurs in the [110] direction with the assistance of capping agents [32]. In our case, the capping agent is Polyvinylpyrrolidone (PVP), which adsorbs on the (100) facet due to its higher surface free energy compared to (111), thereby blocking this facet from further growth. The existing Ag⁰ then adsorbs onto the (111) facet, initiating a continuous process leading to the formation of uniform silver nanowires [22,28,31,33].

In this study, we employed the modified polyol method for synthesizing supported silver nanowires and the incipient wetness method for supported silver spherical particles. Our study delves into the influence of faceting and varied shapes on catalyst activity and selectivity, shedding light on their significant role. Furthermore, we elucidated the impact of heightened oxygen partial pressure on EO selectivity. The morphological changes in silver particles due to annealing and reaction conditions were demonstrated by comparing their structures before and after the reaction. Moreover, the silver nanowires were promoted with Cs, a novel aspect addressed in this study, and were tested for a comparative study against unpromoted catalysts. Notably, the synthesis of silver nanowires proved to be highly sensitive, and our study addressed intricate details often overlooked in existing literature [22,32–34]. We aimed to provide clarity on procedural nuances that are crucial for future studies, aiming to facilitate the reproducibility and understanding of the synthesis process. Our findings underscore that precisely controlled size and shape of catalytic particles not only hold great promise as heterogeneous catalysts for the selective production of chemicals but also serve as a crucial platform for the investigation of heterogeneous catalytic processes.

2. Experiment procedure

The synthesis of silver nanowires is highly sensitive to contaminations, and even the slightest impurity can impact the overall morphology and yield of the nanowires. Therefore, all the beakers and stir bars utilized in the synthesis underwent thorough cleaning procedures involving washing with soap, immersion in a base bath for several days, and triple rinsing with deionized water. Silver nitrate, PVP (Molecular weight: 55,000), ethylene glycol, and hydrochloric acid were procured from Fisher (99.9995 % purity, Cat. No. 010858.14), Sigma (Product No. 856568), Sigma (anhydrous, 99.8 %, Product No. 324558), and Fisher (Certified ACS Plus, Cat. No. A144SI-212), respectively. The alpha aluminum oxide support (Product code SA5562) with 8 mm rings, a surface area of $0.7 \text{ m}^2/\text{g}$, and a pore volume of $0.49 \text{ cm}^3/\text{g}$ was provided by Saint-Gobain company.

2.1. Silver nanowires (AgNWs)

The experimental procedure followed a protocol established in the literature [22], and the schematic of the silver nanowire synthesis is depicted in Fig. 2. Ethylene glycol (25 ml) was placed in a 500 ml round bottom beaker immersed in an oil bath. The stirring rate was set at 300 rpm, and the hot plate temperature was adjusted to achieve an oil bath temperature of 150°C . The temperature difference between the oil bath and the solution was approximately 5°C , resulting in a solution temperature of around 145°C . This temperature was chosen to prevent interference from the thermocouple inside the solution, which could affect the results. The ethylene glycol was stirred at 145°C for 60 minutes with the cap of the round bottom beaker slightly loose to eliminate any potential contaminations. Simultaneously, separate solutions of silver nitrate 0.1 M ($\sim 0.637 \text{ g}$) and PVP 0.375 M (0.625 g) were prepared by dissolving the appropriate amounts in 15 ml of ethylene glycol in separate beakers. The PVP solution required stirring at 35°C to ensure complete dissolution. A 3 mM HCl solution (500 ml) was prepared as a stock solution for all syntheses. After one hour, 1 ml of the 3 mM HCl solution was added at once to the ethylene glycol. Ten minutes later, the solutions of AgNO_3 and PVP were injected into the prepared solution using a syringe pump at a rate of 0.75 ml/min. The

injection rate significantly influenced the morphology of the nanowires. After completing the injection, the cap was tightened, and the reaction continued for 6 hours.

Upon cooling, the gray solution was transferred to plastic centrifuge tubes. To eliminate impurities from the synthesis and separate possible silver particles from the nanowires, the solution underwent three cycles of washing with acetone, DI water, and ethanol in the specified order. Each centrifuge cycle operated at 3000 rpm for 20 minutes. The settled silver nanowires were then dispersed in 5 ml of ethanol and sonicated for 20 minutes to achieve a uniform suspension. In our previous work [27], it was demonstrated that sonication for the specific duration mentioned did not alter the morphology or yield of the silver nanowires. After calcination of the support at 400°C for 3 hours, the rings were ground into particles ranging from $425 \mu\text{m}$ to 1 mm. A mass of 2.56 g of support was contacted with the nanowires' suspension using the wet impregnation method with an excess amount and then dried at 80°C for a few minutes under gentle stirring.

For catalyst promotion, a prepared stock solution of cesium acetate (Sigma, 99 %, Product No. 390831000) in ethanol, with a concentration of 0.376 mM and a total volume of 200 ml, was utilized. Subsequently, enough volume of the cesium acetate solution in ethanol was added stepwise in increments of 1 ml to the supported silver nanowires catalysts. This addition was carried out while maintaining a temperature of 80°C with mild stirring. The resulting promoted catalysts were dried and subsequently calcined at 210°C for 2 hours in an air environment. These prepared catalysts were then employed in the reactor for activity and selectivity testing.

Silver spherical catalysts were synthesized using the incipient wetness method. To create two distinct sizes of spherical catalysts, different references were employed [1,6,18,19]. For the production of larger particles, silver nitrate served as the precursor, and DI water as the solvent was selected. Meanwhile, for the synthesis of smaller particles in the order of diameter comparable to silver nanowires, silver oxalate (Purchased from City Chemicals LLC, 99 %) was chosen as the precursor, and the solvent comprised ethylene diamine (Purchased from Sigma, Product No. 8.00947) and DI water. In the case of larger particles, an ample quantity of silver nitrate, sufficient for producing 5 g of catalysts with a 10 wt% Ag content, was dissolved in 10–15 ml of DI

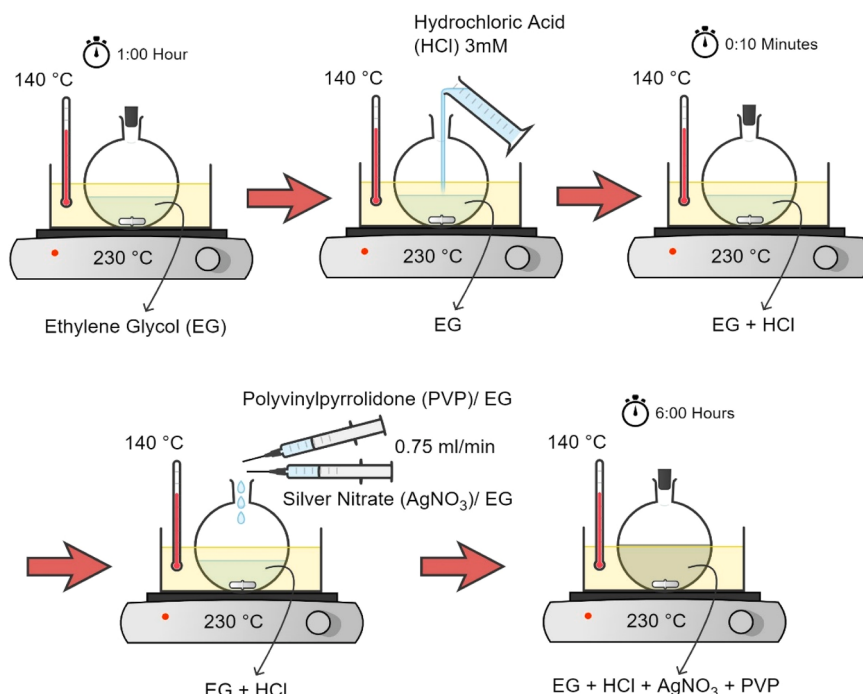


Fig. 2. Schematic of Modified Polyol Method for Silver Nanowires Synthesis.

water and stirred at room temperature. Subsequently, the solution was added dropwise to the 8 mm rings of the support while being heated at 80°C on a hot plate without stirring to prevent damage to the supports. The beakers were shaken instead of stirred to avoid damage to the rings while also achieving a uniform distribution of silver particles. After complete drying, the samples were transferred to a crucible and calcined in an oven at 400°C for 3 hours, with a ramping rate of 5 °C/min in stagnant air. For the smaller silver spherical catalysts, a 200 ml stock solution of ethylenediamine (EN) and DI water was initially prepared with a ratio of 0.73 g/g of EN to water. To create 5 g of catalysts, an appropriate amount of silver oxalate for achieving 5 wt% and 10 wt% silver content was dissolved in 2 and 4 ml of the EN/water solution, respectively. The samples were heated on a hot plate at 60°C without stirring to prevent damage to the supports. Following complete evaporation, the samples were transferred into crucibles and calcined in the oven at 215°C for 4 hours with a ramping rate of 5 °C/min in a stagnant air atmosphere. After impregnation, the catalysts were ground to a particle size between 425 µm and 1 mm and subsequently tested for reaction activity and selectivity.

3. Characterization and reactor setup

Scanning electron microscopy (SEM) analysis was conducted utilizing a Zeiss Gemini 500 equipped with a secondary electron detector (SE2). The supported silver catalysts were affixed to carbon-backed adhesive tape and coated with a thin layer of gold using a Denton Desk II sputter coater with global rotation and tilt. In the case of unsupported silver nanowires, a single drop of the suspension was deposited onto the carbon-backed adhesive tape and allowed to dry for a few days. SEM images were acquired using an SE2 detector at a beam energy of 15 kV.

Inductively coupled plasma-optical emission spectroscopy (ICP-OES, Perkin Elmer Avio 200) was employed for elemental analyses, utilizing periodically collected aliquots from liquid samples. Vessels, tubing, and the pump liner were constructed from inert materials such as plastic or Teflon, and they underwent meticulous cleaning with 37 % nitric acid, followed by thorough rinsing with deionized water between sample analyses.

Chemisorption experiments were conducted involving the titration of hydrogen (H₂) on a silver surface previously covered with oxygen (O₂). The experiments utilized a Micromeritics 2920 pulsed chemisorption analyzer, following a procedure outlined in the literature [35]. The sample preparation involved the reduction of silver samples for 2 hours at 280°C in a gas mixture containing 10 % H₂ and the remainder Ar. Subsequently, the samples were cooled to 180°C and purged with flowing Ar for 30 minutes to remove H₂. Afterward, they were exposed to a gas mixture consisting of 10 % O₂ balanced with He for 30 minutes to saturate the silver surface with oxygen. Ar flowed for 30 minutes to remove the extra gaseous oxygen. The pulsed H₂ titration was then conducted at 170°C. The ratio of oxygen pre-covered silver surface to hydrogen was set at 1:1. Each sample underwent an additional sequence of H₂ titration, and the results are reported as an average.

The reactor employed a 3/8" stainless steel tube housing 1 g of α-Al₂O₃-supported catalyst powder, with temperature monitored using a K-type thermocouple positioned within the catalyst bed. The experimental setup involved three distinct gas cylinders: one containing 20 % Ethylene in Nitrogen, another with Pure Oxygen, and the third with Pure Nitrogen (All gases were of UHP purity grade, with most purchased from Airgas, except for the ethylene/nitrogen mixture, which was obtained from Praxair). For experimental runs, the feed compositions were adjusted to maintain a constant 10 % ethylene concentration while varying the oxygen concentration to achieve 10 %, 30 %, and 50 % levels. This was achieved by adjusting the flow rates of nitrogen and oxygen while keeping the ethylene flow rate constant. Throughout these experiments, the total flow rate was consistently set at 20 sccm. Effluent analysis was conducted through a Shimadzu 2014 Gas Chromatograph

(GC) equipped with Q Plot and ShinCarbon columns, linked to flame ionization (FID) and thermal conductivity (TCD) detectors, respectively. Electrical heat tape was utilized to wrap the effluent lines to prevent the ingress of liquids into the GC. All the reaction results presented in this paper were obtained after the EO and ethylene concentrations stabilized, ensuring that selectivity and ethylene conversion were measured under stable conditions.

4. Results and discussion

In Fig. 3(a), the unsupported silver nanowires, synthesized using a modified polyol method, are depicted. The majority of silver nanowires appeared straight, with lengths of up to 30 µm. The diameter distribution of these nanowires is illustrated in Fig. 3(b) through a histogram, revealing an average diameter of 218 nm with a relatively narrow distribution. Comparing the histogram of the silver nanowires synthesized with the modified polyol method in this study to the silver nanowires synthesized with the hydrothermal method in our previous study [27], thicker nanowires were observed with the modified polyol method, as the hydrothermal method yielded an average below 100 nm.

The end and side edges of individual nanowires are further presented in Fig. 4(a) and (b). Consistent with existing literature [31], both ends of the nanowires exhibit the (111) facet, while the side edges feature the (100) facet. Additionally, Fig. 4(a) showcases the [110] direction, indicating the growth direction of the nanowires. As indicated in this figure, the nanowires have (100) facets on the side edges and (111) facets at both ends. Considering the long length of these nanowires, the side edges have a greater surface area compared to the ends, indicating that the majority of the surface area is composed of (100) facets. Fig. 4 (b) depicts the light contrast on the edges of a single silver nanowire. For further clarification, two different surfaces are delineated by two red

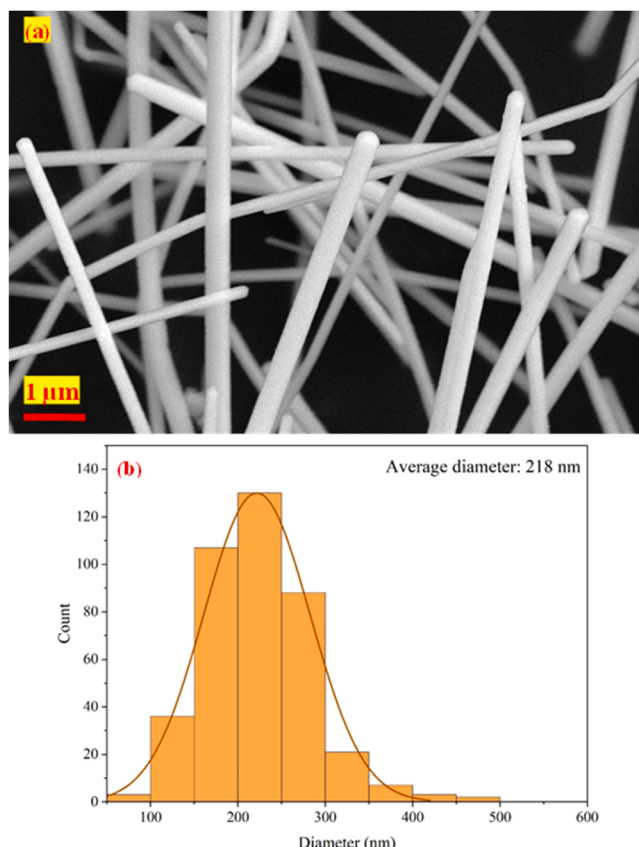


Fig. 3. (a) SEM image of unsupported silver nanowires (AgNWs) synthesized by modified polyol method. (b) Histogram of silver nanowires.

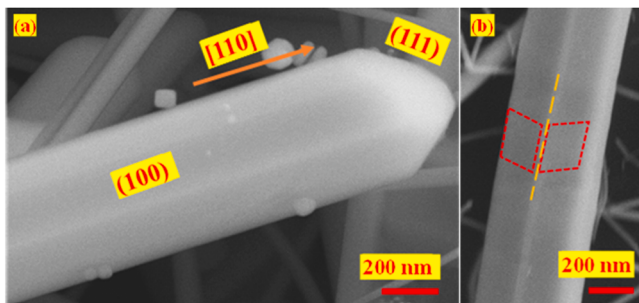


Fig. 4. (a) SEM image of the end of a single silver nanowire, illustrating distinct crystal faceting. (b) SEM image of the sides of a single silver nanowire, highlighting the cross-sectional morphology and surface features along its length.

rectangles. The lighter part, representing the edge connecting these two different surfaces, is indicated by a yellow line. This light contrast on the side of a single silver nanowire reveals a non-circular cross-section. As mentioned previously and according to the literature [36,37], the silver seeds/MTPs forming the silver nanowires have a decahedral shape with a pentagon cross-section, indicating that the nanowires share the same cross-sectional shape.

To prepare the silver nanowires as catalysts for chemical reactions, wet impregnation was employed to deposit the synthesized silver nanowires onto the $\alpha\text{-Al}_2\text{O}_3$ support. The settled silver nanowires were sonicated in ethanol to form a suspension, then contacted with the support in an amount to achieve a 10 wt% loading of silver nanowires on the support. The samples were subsequently dried at 80°C with gentle stirring and characterized using SEM and ICP. In Fig. 5, the SEM image illustrates the morphology of silver nanowires after impregnation onto the support. The nanowires are uniformly distributed across the surface of the support. Importantly, the overall morphology of the nanowires remains unchanged following sonication, drying, and mild stirring. ICP analysis revealed approximately 5 wt% of silver on the support, indicating significant loss of silver during the preparation process. This waste could occur at various stages, such as during nanowire synthesis, where some nanowires may adhere to the bottom of the round-neck flask, during centrifugation, where any potential synthesized spherical particles are separated from the nanowires, and during impregnation, where a small portion of nanowires may stick to the beaker. The use of ethanol as a solvent for impregnating silver nanowires onto the support is deemed essential for preserving their structure [22,24]. Although investigating the scientific reasons for using ethanol as a solvent was beyond the scope of this study, our previous research has shown that

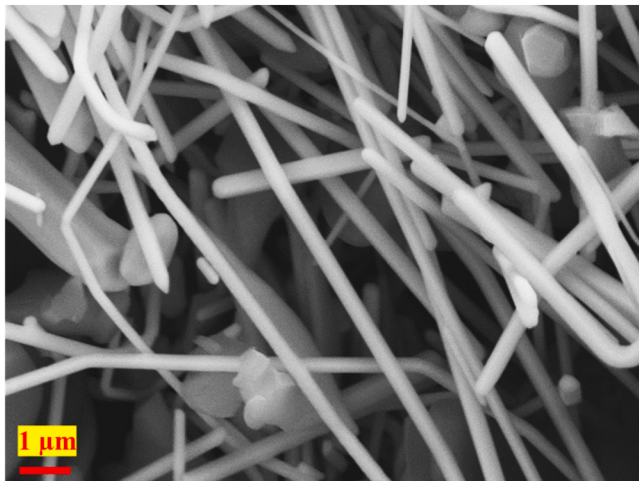


Fig. 5. SEM image of uniformly distributed silver nanowires on $\alpha\text{-Al}_2\text{O}_3$ support with 5 wt% silver loading.

using water as a solvent resulted in nanowires sticking to each other rather than to the support [28].

Silver spherical particles were synthesized using wet impregnation methods, employing two different silver precursors and sets of solvents to produce particles of two different sizes. Using silver nitrate and DI water as the silver precursor and solvent would not result in a narrow distribution and small particles, as shown in the references used for synthesis [6,38,39]. Therefore, the spherical particles synthesized using silver nitrate and DI water via wet impregnation in this study are referred to as larger silver spherical particles. In Fig. 6(a) and (b), SEM images depict larger silver spherical catalysts supported on $\alpha\text{-Al}_2\text{O}_3$, along with a histogram illustrating the diameter distribution. The diameter distribution is broad, with an average diameter calculated at 786 nm. On the other hand, using silver oxalate, which has a lower decomposition temperature, and a mixture of ethylenediamine and DI water resulted in smaller silver particles via the wet impregnation synthesis method. Ethylenediamine acts as both the solvent for silver oxalate and plays a surfactant-like role necessary for better distribution and smaller silver particles [18,35,40]. Moving to Fig. 7(a) and (b), SEM showcases smaller silver spherical particles distributed on $\alpha\text{-Al}_2\text{O}_3$, accompanied by a histogram indicating a narrower distribution and an average diameter of 211 nm. The particle size ranges for both large and small sizes align with literature values utilized during synthesis [35,39,40]. This observation underscores the potential influence of the silver precursor, choice of solvents, and calcination time and temperature on the size and distribution of silver particles.

Following the synthesis of the silver nanowires and spherical particles as representatives of Ag(100) and Ag(111), respectively, all the catalysts were tested for the EPO reaction under similar conditions. The

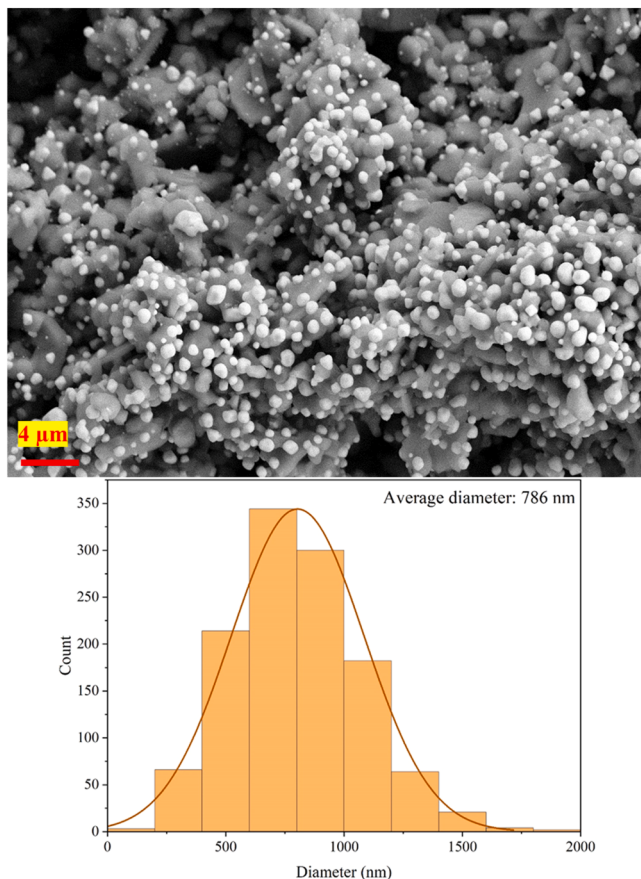


Fig. 6. (a) SEM image of large silver spherical particles supported on $\alpha\text{-Al}_2\text{O}_3$, synthesized using the wet impregnation method. (b) Particle size distribution histogram of silver spherical particles, showing an average diameter of 786 nm.

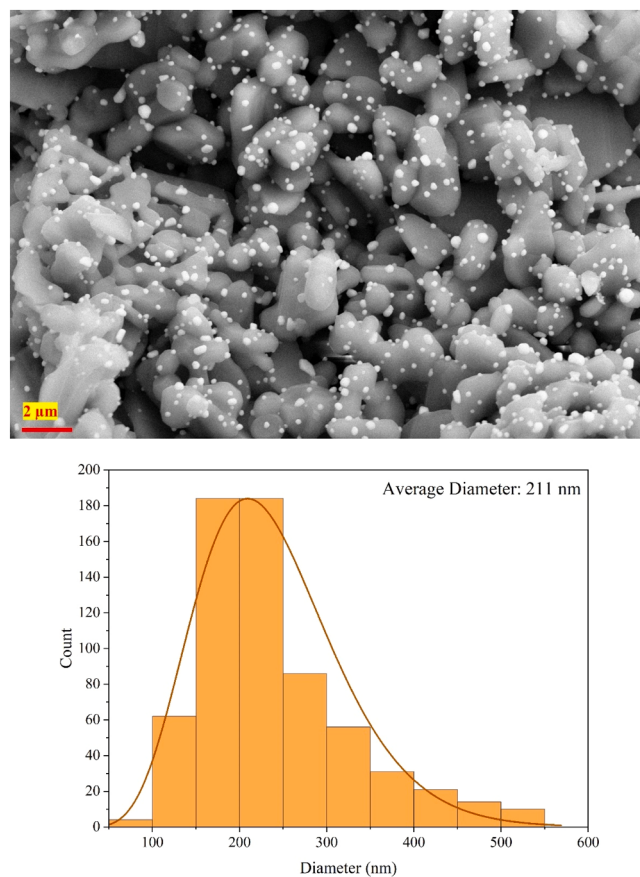


Fig. 7. (a) SEM image of small silver spherical particles supported on α -Al₂O₃. (b) Particle size distribution histogram of silver spherical particles, showing an average diameter of 211 nm.

space velocity was maintained at approximately 4700 1/hr, with bed temperatures ranging from 200°C to 260°C, and the reaction was conducted at atmospheric pressure. The ethylene concentration remained constant, while oxygen and nitrogen concentrations were adjusted to achieve three different ethylene-to-oxygen ratios: 1–1, 1–3, and 1–5. For all catalysts and ethylene-to-oxygen ratios, the furnace temperature was adjusted to maintain a constant 10 % ethylene conversion, and the EO selectivity was compared for each data point. As previously shown, EO selectivity does not change linearly with conversion [1]. Therefore, we maintained the ethylene conversion at a constant 10 % to facilitate a fair comparison between our synthesized catalysts and the benchmark catalysts, which were also tested at 10 % conversion [18]. This ensured that differences in selectivity were due to catalyst performance rather than conversion effects. Although adjusting the flow rates would have been ideal for controlling conversion, the limitations of the low reactant flow rates and the mass flow controllers (MFCs) in our setup made temperature adjustment necessary. Moreover, adjusting the feed conditions to enable a fair comparison is common in EPO reaction. Previous research has shown that performance can vary even within the same batch of catalysts, making the comparison of EPO catalysts particularly challenging [6]. Common methods used in the literature to address this include adjusting the temperature or maintaining a low conversion to report results over a range of conversion values [16,19,22,39,41]. The EO selectivity of AgNWs compared to four different AgSPs catalysts is depicted in Fig. 8. Regardless of shape, increasing the oxygen partial pressure resulted in an increase in EO selectivity for all silver catalysts due to the positive reaction order with respect to oxygen in EO formation [6,22,42]. Three different silver spherical catalysts were synthesized, with two of them having 10 wt% silver, considered the optimal

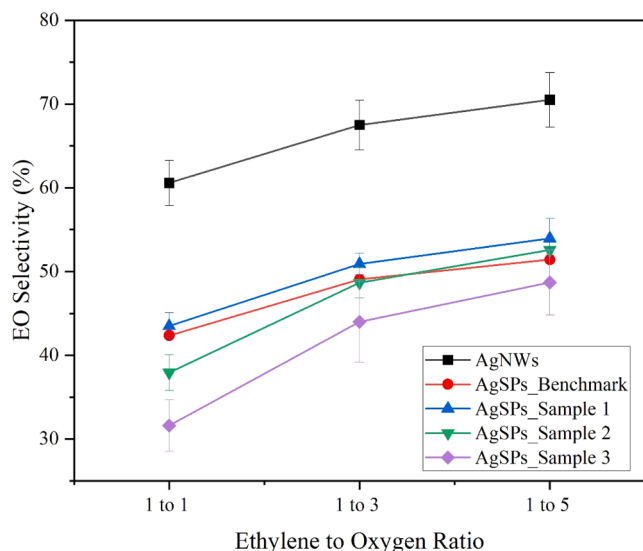


Fig. 8. EO selectivity of various silver-shaped catalysts at different ethylene-to-oxygen ratios, maintaining a constant 10 % ethylene conversion. AgNWs: 5 wt % silver nanowires on α -Al₂O₃; AgSPs_Benchmark: 10–12 wt% silver on α -Al₂O₃ (as reported in the literature [17,37]); AgSPs_Sample 1: 10 wt% silver spherical particles on α -Al₂O₃ with an average diameter of 211 nm; AgSPs_Sample 2: 5 wt% silver spherical particles on α -Al₂O₃ with an average diameter of 211 nm; AgSPs_Sample 3: 10 wt% silver spherical particles on α -Al₂O₃ with an average diameter of 786 nm.

loading for the EPO reaction [6,18]. These catalysts comprised smaller and larger silver particles, named AgSPs_Sample 1 and AgSPs_Sample 3, respectively. Upon comparing the EO selectivity of these two catalysts, AgSPs_Sample 1 exhibited higher EO selectivity than AgSPs_Sample 3 for all ethylene-to-oxygen ratios at the same ethylene conversion. This finding contrasts with a study by Christopher et al. [22], which compared spherical particle catalysts of sizes 100 nm and 1 μ m. However, some studies [1,43] have shown that an average particle size closer to 140 nm exhibits the highest EO rate compared to both larger and smaller particles, similar to our observations. To find the reason for this discrepancy in Christopher et al.'s study, the silver active sites of each catalyst were calculated using oxygen-recovered hydrogen pulse chemisorption and summarized in Table 1. The silver active sites for AgSPs_Sample 1 are almost 6 times greater compared to AgSPs_Sample 3, explaining the higher EO selectivity. A crucial aspect to consider in elucidating the disparity between our study and the referenced one is the differing synthesis methods employed for the smaller and larger spherical catalysts in the referenced study. Specifically, the smaller particles were synthesized using the modified polyol method with the capping agent, whereas the larger ones were synthesized via wet impregnation without the use of any capping agent [22]. According to literature reports [32,44], the capping agent cannot be completely removed from the silver surface, which could affect the number of active sites of the smaller catalyst in the mentioned study and may explain why the smaller catalyst exhibited lower EO selectivity. Given the ICP results for AgNWs catalysts indicating 5 wt% silver on the surface of aluminum oxide, a 5 wt% silver spherical catalyst within the same nanowire diameter range was synthesized and named AgSPs_Sample2. This catalyst displayed lower EO selectivity compared to AgSPs_Sample 1 due to fewer active sites and lower silver weight loading, as indicated in Table 1. A benchmark catalyst, supplied by another group and whose results were published in the literature [18,40], was also tested in our setup for verification and comparison. The EO selectivity of the benchmark catalyst, indicated by the red line in Fig. 8, closely matched that of our AgSPs_Sample 1, verifying both our catalysts and setup.

Comparing the spherical catalysts to the AgNWs catalyst, indicated by the black line, it is evident that AgNWs exhibited higher EO

Table 1

Oxygen pre-covered hydrogen chemisorption results for various silver catalysts.

Catalyst	H ₂ uptake (cm ³ /g)	Active sites (per g catalyst)	Active sites (per g metal)	Particle size Chemisorption (nm)	Particle Size SEM (nm)
10 wt% Ag/α-Al ₂ O ₃ (AgSPs_Sample1)	0.095	2.55E+ 18	2.55E+ 19	215	211
5 wt% Ag/α-Al ₂ O ₃ (AgSPs_Sample2)	0.044	1.18E+ 18	2.37E+ 19	231	211
10 wt% Ag/α-Al ₂ O ₃ (AgSPs_Sample3)	0.016	4.33E+ 17	4.33E+ 18	1265	786
5 wt% AgNWs/α-Al ₂ O ₃	0.038	9.2E+ 17	2.2E+ 19	N/A	218

selectivity significantly at all the ethylene-to-oxygen ratios. This is attributed to the higher concentration of (100) facet compared to (111) facet in the silver nanowires catalysts, confirming that Ag(100) has higher EO selectivity and activity than Ag(111) for EO, as previously demonstrated in computational and experimental studies [20,22]. Comparing the number of active sites per metal basis across various catalysts, as detailed in Table 1, unveils the remarkable superiority of silver nanowires in terms of selectivity, despite having a similar count of active sites. It should be highlighted that, as previously mentioned, the catalyst bed temperature was adjusted to maintain a constant ethylene conversion. A comparison of the bed temperatures for the three top-performing catalysts—Benchmark, AgNWs, and AgSPs_Sample 1—illustrated in Fig. S2, shows that all three catalysts operated under nearly identical bed temperatures at each oxygen partial pressure. As a result, the EO selectivities of these catalysts were compared under identical conditions of temperature, pressure, and ethylene conversion at each oxygen partial pressure, ensuring a fair evaluation of their performance. This underscores the pronounced EO selectivity of Ag(100) over Ag(111), as mentioned previously, highlighting the significant difference in selectivity between the two crystal facets.

The EO formation rate per gram of catalyst is presented in Fig. 9 for AgNWs and the best-performing silver spherical catalysts in our study to compare the activity. Notably, despite AgNWs having less than half the silver loading compared to the spherical catalysts, they exhibited significantly higher EO formation rates. These rates were measured under the same temperature, pressure, and ethylene conversion conditions, further highlighting that AgNWs, and specifically the Ag(100) facets, demonstrated higher EO formation rates compared to the spherical catalysts and Ag(111) facets. Therefore, the AgNWs catalyst

not only showed higher EO selectivity but also higher activity despite having fewer silver sites at similar operational conditions compared to the AgSPs catalyst. Although the number of silver active sites is provided in Table 1, we have not reported the TOF due to a critical consideration. The silver nanowires do not consist purely of (100) facets; as mentioned previously, both ends of a single silver nanowire feature (111) facets. Additionally, there are defect sites along the edges of the nanowires where the surfaces converge [22]. These facets exhibit different oxygen adsorption and reaction rates [20]. Therefore, the values obtained by chemisorption may not accurately reflect the number of active silver sites responsible for ethylene oxide production. Moreover, since neither the nanowires nor the spherical particles are composed purely of (100) or (111) facets, TOF would not provide a precise comparison of the activity of these facets. For this reason, we opted to compare EO selectivity and EO formation rates at constant ethylene conversion to ensure a fair comparison of catalyst performance.

As mentioned previously, cesium is widely recognized as an effective promoter for silver catalysts in the epoxidation reaction of ethylene. While there have been limited studies on cesium-promoted silver nanowires for styrene epoxidation [34,45], our study is the first comprehensive investigation for promoting silver nanowires with cesium and testing their efficacy in the epoxidation of ethylene. Promoting silver particles with cesium for the EPO reaction should be at the ppm level, to avoid blocking silver sites [8,18]. Three different loadings of cesium were employed to explore the EO selectivity of promoted silver nanowires and determine the optimal cesium loading for the AgNWs catalyst. Additionally, small and large 10 wt% silver spherical catalysts, AgSPs_Sample 1 and AgSPs_Sample 3, were also subjected to cesium promotion with optimal loadings based on existing literature [8,18,40], facilitating a comprehensive comparison of all catalyst activities. All the promoted silver catalysts were tested under similar feed conditions and ethylene-to-oxygen ratios at various bed temperatures to maintain a 10 % ethylene conversion for all the catalysts and ratios. Fig. 10 illustrates the EO selectivity for various amounts of cesium-promoted silver nanowires as a function of ethylene-to-oxygen ratios. No reduction was performed during pretreatment, as reducing conditions could potentially lead to silver nanowire sintering. Importantly, cesium serves a similar function in enhancing EO selectivity even if oxidized into CsO [14]. Increasing the oxygen partial pressure resulted in a corresponding increase in EO selectivity, mirroring the behavior observed with unpromoted silver catalysts. The trend of increasing EO selectivity with promoted AgNWs was comparable to that of the unpromoted catalysts. Cesium is believed to enhance EO selectivity by inducing dipole moments, reducing the energy barrier for O₂ dissociation, and stabilizing intermediates for EO formation, as discussed previously [14–17].

To investigate the effect of different Cs loadings, Fig. 11 illustrates the EO selectivity of various promoted silver nanowires as a function of cesium loading. Increasing the Cs amount to 66 ppm and 133 ppm resulted in a further enhancement of EO selectivity compared to the unpromoted catalyst. However, at a 200-ppm loading, the EO selectivity was lower than that of the unpromoted sample. Despite the lower selectivity of 200-ppm Cs promoted AgNWs compared to unpromoted AgNWs, this selectivity still surpassed that of the spherical catalyst. It is worth noting that a further addition of cesium loading was tested, which resulted in a deactivated catalyst. This deactivation occurs because

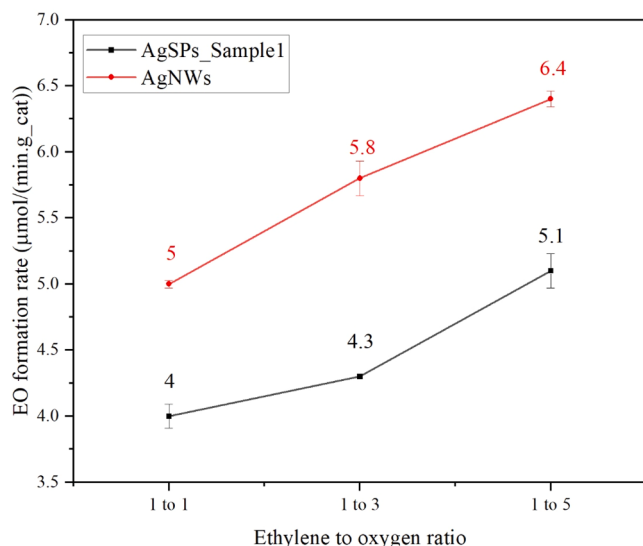


Fig. 9. EO formation rate for unpromoted AgNWs and AgSPs_Sample1 at three different ethylene to oxygen ratios. AgNWs: 5 wt% unpromoted silver nanowires on α-Al₂O₃; AgSPs_Sample 1: 10 wt% silver spherical particles on α-Al₂O₃ with an average diameter of 211 nm.

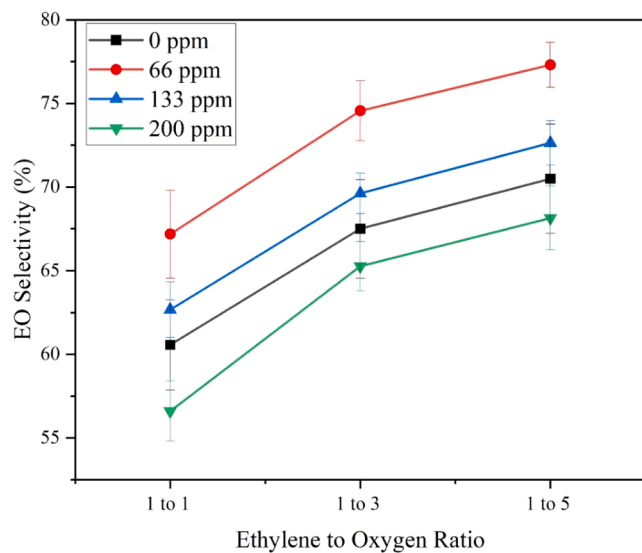


Fig. 10. EO selectivity of Cs-promoted 5 wt% silver nanowires with varying Cs loadings as a function of ethylene-to-oxygen ratios, at a constant 10 % ethylene conversion.

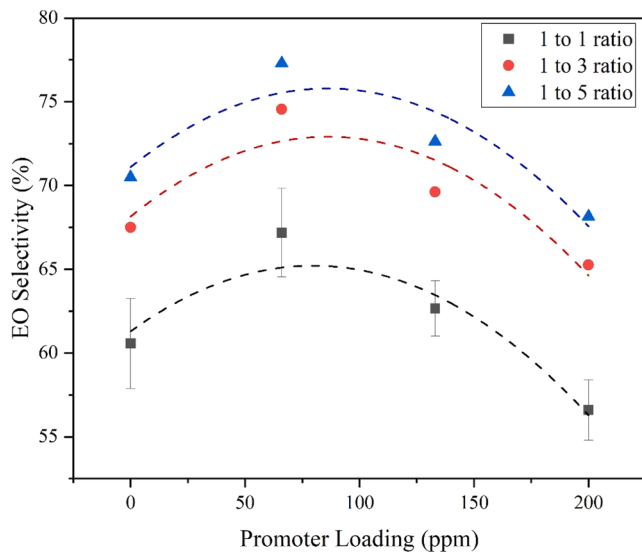


Fig. 11. EO selectivity of Cs-promoted 5 wt% silver nanowires as a function of cesium loading at a constant 10 % ethylene conversion and varying ethylene-to-oxygen ratios.

cesium, being a large atom, cannot easily diffuse into the silver particles. Consequently, adding high amounts of cesium could block the silver active sites, thereby reducing the catalyst's selectivity. Moreover, it has been reported that high Cs loading can transform oxygen atoms into nucleophilic species, leading to the combustion of ethylene and the formation of more undesirable by-products [41]. Therefore, similar to spherical catalysts reported in the literature [8,16,18], there exists an optimal cesium loading for silver nanowires. Although the experiment's design was not conducted in this study, it is anticipated that the optimal Cs loading would be close to 66 ppm for silver nanowires.

A comparison of the EO selectivity of both unpromoted and promoted silver nanowires, alongside unpromoted and promoted 10 % silver spherical particles of two different sizes, is presented in Fig. 12. The 10 % AgSPs catalysts were chosen to compare the best spherical catalysts to our nanowire samples. AgSPs_Sample 1 was promoted with 350 ppm of cesium, and AgSPs_Sample 3 was promoted with 70 ppm,

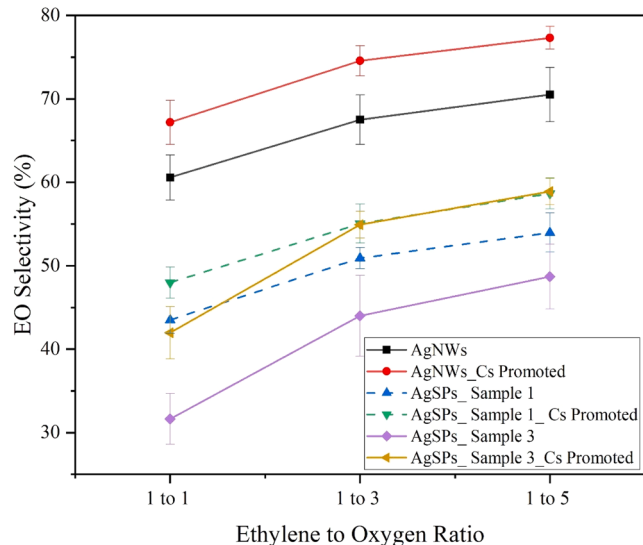


Fig. 12. EO selectivity of unpromoted and Cs-promoted silver catalysts at different ethylene-to-oxygen ratios, maintaining a constant 10 % ethylene conversion. AgNWs: 5 wt% unpromoted silver nanowires on $\alpha\text{-Al}_2\text{O}_3$; AgNWs_Cs Promoted: 5 wt% Cs-promoted silver nanowires with 66 ppm Cs loading on $\alpha\text{-Al}_2\text{O}_3$; AgSPs_Sample 1: 10 wt% silver spherical particles on $\alpha\text{-Al}_2\text{O}_3$ with an average diameter of 211 nm; AgSPs_Sample 1_Cs Promoted: 10 wt% Cs-promoted small silver spherical particles with optimal Cs loading (350 ppm, as reported in the literature [17]) on $\alpha\text{-Al}_2\text{O}_3$; AgSPs_Sample 3: 10 wt% silver spherical particles on $\alpha\text{-Al}_2\text{O}_3$ with an average diameter of 786 nm; AgSPs_Sample 3_Cs Promoted: 10 wt% Cs-promoted large silver spherical particles with optimal Cs loading (70 ppm, as reported in the literature [7]) on $\alpha\text{-Al}_2\text{O}_3$.

following the literature [8,18], utilizing the same precursor and treatment conditions as the AgNWs samples. Moreover, among the different cesium loadings of AgNWs samples, the 66-ppm level was selected as the best-promoted AgNWs sample in Fig. 12. Across all the catalysts tested in this study and across all ethylene-to-oxygen ratios, the promoted AgNWs catalyst exhibited the highest EO selectivity, reaching nearly 80 % at a 1-to-5 ratio of ethylene to oxygen with 10 % ethylene conversion. Notably, the best-promoted silver spherical catalysts with 10 wt % silver loading demonstrated lower EO selectivity compared to even the unpromoted AgNWs with approximately 5 wt% silver, highlighting the high activity and selectivity of silver nanowires. The promoted AgNWs and AgSPs exhibited a 20 % difference in EO selectivity.

The EO selectivity of AgNWs catalysts has been compared with literature findings to provide understanding of their efficacy in this field. Literature reports indicate variability in silver catalyst activity and selectivity between batches [6], and direct comparison of catalyst performance under identical conditions across studies is challenging. Thus, a curated summary of literature data, including operating conditions, catalysts, and feed compositions, is presented in Table 2. Initially, a comparison was made between our unpromoted AgNWs (entries 26–28) and unpromoted, non-chloride (Cl)-added spherical catalysts (entries 1–14). Notably, AgNWs exhibited higher EO selectivity despite achieving higher ethylene conversion and possessing 5 wt%-10wt% less silver loading compared to all unpromoted spherical catalysts. While EO selectivities of AgNWs from our study and those in the literature (entries 23–28) fell within a similar range, differences in ethylene conversion suggest higher yields with lower silver loading in our study. These disparities may be attributed to varying space velocity, nanowire diameter, and other unresolved factors that inspire further investigation. Although chloride was not utilized in this study, a comparison between results from Cl-added (entry 4) and non-Cl-added studies (entry 21) reveals observable effects of Cl on EO selectivity at constant ethylene conversion. Subsequently, promoted Cl-added AgSPs (entry 22) were compared

Table 2

Comparative analysis of catalytic EO selectivity.

No.	Catalysts	Feed composition	Bed temperature	Pressure	Silver weight loading	Silver particle size	Promoter/feed additive	Conversion (%)	Selectivity (%)	Reference
1	Ag/Al ₂ O ₃	Ethylene/Oxygen= 1:1	217°C	1 atm	11–13 %	10–20 μm	—	1.81	32	[8]
2	Ag/Al ₂ O ₃	Ethylene/Oxygen= 1:3	217°C	1 atm	11–13 %	10–20 μm	—	2.18	38	[8]
3	Ag/Al ₂ O ₃	Ethylene/Oxygen= 1:5	217°C	1 atm	11–13 %	10–20 μm	—	2.97	41	[8]
4	Ag/Al ₂ O ₃	Ethylene/Oxygen= 3:1	230°C	1 atm	15 %	90 nm	—	10	38	[1]
5	Ag/Al ₂ O ₃	Ethylene/Oxygen= 1:1	290°C	1 atm	15 %	50 nm	—	5	38.5	[46]
6	Ag/Al ₂ O ₃	Ethylene/Oxygen= 1:1	237°C	1 atm	10 %	100 nm	—	2–4	32	[22]
7	Ag/Al ₂ O ₃	Ethylene/Oxygen= 1:3	237°C	1 atm	10 %	100 nm	—	2–4	38	[22]
8	Ag/Al ₂ O ₃	Ethylene/Oxygen= 1:5	237°C	1 atm	10 %	100 nm	—	2–4	40	[22]
9	Ag/Al ₂ O ₃	Ethylene/Oxygen= 1:1	237°C	1 atm	10 %	1 μm	—	2–4	38	[22]
10	Ag/Al ₂ O ₃	Ethylene/Oxygen= 1:3	237°C	1 atm	10 %	1 μm	—	2–4	44	[22]
11	Ag/Al ₂ O ₃	Ethylene/Oxygen= 1:5	237°C	1 atm	10 %	1 μm	—	2–4	47	[22]
12	Ag/Al ₂ O ₃	Ethylene/Oxygen= 1:1	230°C	1 atm	15 %	50–200 nm	—	5	28	[19]
13	Ag/Al ₂ O ₃	Ethylene/Oxygen= 1:1	290°C	1 atm	15 %	44 nm	—	4.6	38.5	[46]
14	Ag/Al ₂ O ₃	Ethylene/Oxygen= 3.5:1	200°C	1 atm	15 %	160 nm	—	3.07	35.6	[47]
15	Ag/Al ₂ O ₃	Ethylene/Oxygen= 1:1	217°C	1 atm	11–13 %	10–20 μm	68 ppm Cs	1–3	46	[8]
16	Ag/Al ₂ O ₃	Ethylene/Oxygen= 1:3	217°C	1 atm	11–13 %	10–20 μm	68 ppm Cs	1–3	53	[8]
17	Ag/Al ₂ O ₃	Ethylene/Oxygen= 1:5	217°C	1 atm	11–13 %	10–20 μm	68 ppm Cs	1–3	56	[8]
18	Ag/Al ₂ O ₃	Ethylene/Oxygen= 1:1	217°C	1 atm	11–13 %	10–20 μm	68 ppm Cs, 1 ppm Cl	1–3	60	[8]
19	Ag/Al ₂ O ₃	Ethylene/Oxygen= 1:3	217°C	1 atm	11–13 %	10–20 μm	68 ppm Cs, 1 ppm Cl	1–3	62	[8]
20	Ag/Al ₂ O ₃	Ethylene/Oxygen= 1:5	217°C	1 atm	11–13 %	10–20 μm	68 ppm Cs, 1 ppm Cl	1–3	64	[8]
21	Ag/Al ₂ O ₃	Ethylene/Oxygen= 3:1	224°C	17 atm	12 %	120 nm	1–3 ppm Cl	10	74	[18]
22	Ag/Al ₂ O ₃	Ethylene/Oxygen= 3:1	224°C	17 atm	12 %	120 nm	350 ppm Cs, 1–3 ppm Cl	10	79	[18]
23	AgNWs/Al ₂ O ₃	Ethylene/Oxygen= 1:1	237°C	1 atm	10 %	125 nm	—	2–4	50	[22]
24	AgNWs/Al ₂ O ₃	Ethylene/Oxygen= 1:3	237°C	1 atm	10 %	125 nm	—	2–4	62	[22]
25	AgNWs/Al ₂ O ₃	Ethylene/Oxygen= 1:5	237°C	1 atm	10 %	125 nm	—	2–4	65	[22]
26	AgNWs/Al ₂ O ₃	Ethylene/Oxygen= 1:1	200–260°C	1 atm	5 %	218 nm	—	10	61	This Study
27	AgNWs/Al ₂ O ₃	Ethylene/Oxygen= 1:3	200–260°C	1 atm	5 %	218 nm	—	10	67	This Study
28	AgNWs/Al ₂ O ₃	Ethylene/Oxygen= 1:5	200–260°C	1 atm	5 %	218 nm	—	10	70	This Study
29	AgNWs/Al ₂ O ₃	Ethylene/Oxygen= 1:1	200–260°C	1 atm	5 %	218 nm	66 ppm Cs	10	67	This Study
30	AgNWs/Al ₂ O ₃	Ethylene/Oxygen= 1:3	200–260°C	1 atm	5 %	218 nm	66 ppm Cs	10	74	This Study
31	AgNWs/Al ₂ O ₃	Ethylene/Oxygen= 1:5	200–260°C	1 atm	5 %	218 nm	66 ppm Cs	10	77	This Study

with our promoted, non-Cl-added AgNWs (entries 29–31). The ethylene oxide selectivities of AgNWs in this study were comparable to those of the AgSPs catalyst (entry 22), which is recognized in the literature as one of the most active catalysts for ethylene epoxidation. However, several important distinctions between these two catalysts should be noted. Notably, the AgSPs catalyst used in entry 22 had a 7 % higher silver loading and was tested under higher total pressure compared to the AgNWs. This variation in silver loading likely plays a crucial role in catalyst performance. As demonstrated in Fig. S3, the unpromoted 10 wt

% AgNWs achieved over 80 % EO selectivity at high oxygen partial pressures—more than 10 % higher than the unpromoted 5 wt% AgNWs shown in Fig. 12. Furthermore, AgNWs exhibited lower optimal Cs loadings relative to the AgSPs in entry 22. Additionally, as shown in Table 2, the addition of Cl was found to significantly enhance EO selectivity. It is important to note that none of the experiments in this study included Cl in the feed, allowing for an assessment of catalyst performance without the influence of chlorine-induced surface modifications. Given that Cl can alter surface structure, baseline studies such as

this are essential for isolating the intrinsic properties of the catalysts. Therefore, incorporating Cl into the AgNWs, in conjunction with the use of 10 wt% AgNWs, could potentially lead to even greater improvements in EO selectivity than those reported in Table 2. These results underscore the high EO selectivity of Cs-promoted AgNWs, suggesting that further enhancement may be possible through Cl addition and increased silver loading in future studies.

One unexplored aspect in the existing literature pertaining to experiments conducted on the (100) facets of silver involves the investigation of time-on-stream stability. In particular, the ethylene epoxidation reaction necessitates a relatively extended period at the onset of the run to achieve a stable state. Numerous studies on spherical silver catalysts have reported a time frame of 24–72 hours for this reaction to attain stability [8,18,22,40]. Fig. 13 illustrates the EO selectivity for unpromoted silver nanowires from the initiation up to 48 hours of continuous operation. Notably, the EO selectivity stabilizes after approximately 10–15 hours, considerably lower than the 24–72 hours required for spherical catalysts to achieve stability, as mentioned in the literature. Moreover, the EO selectivity of AgNWs after reaching the stable point remained consistent, indicating good stability compared to the findings reported in the literature [22], where the EO selectivity dropped between 3 % and 5 % after a few hours. In an extended run, not depicted here, it was observed that the EO selectivity of silver nanowires experienced a decline of only 3 %–5 % after 10 days of continuous operation. This observation may be attributed to the larger diameter of the AgNWs utilized in our study. It is well-established that a direct correlation exists between diameter size and sintering time within the reaction environment [48]. Consequently, the larger the diameter, the longer the particles will persist within the stream [48].

The absence of discussion on the morphological alterations of AgNWs in certain studies [34,45], coupled with observed deformations in investigations of spent catalysts after a few hours of exposure to the reaction environment [22,24], underscores the significance of understanding the stability and morphology of AgNWs. Thus, to address this gap, we present a morphological analysis of our samples in the SEM image depicted in Fig. 14. After 50 hours on the stream, the AgNWs remained unchanged on the support, demonstrating robust stability and resistance to sintering. This observation aligns with the EO selectivity results, which showed no decrease in EO selectivity. In the inset, a solitary nanowire with a reduced diameter at its midpoint is observed, a characteristic indicative of the Necking phenomenon [48]. This observed Necking phenomenon elucidates the sintering dynamics of the

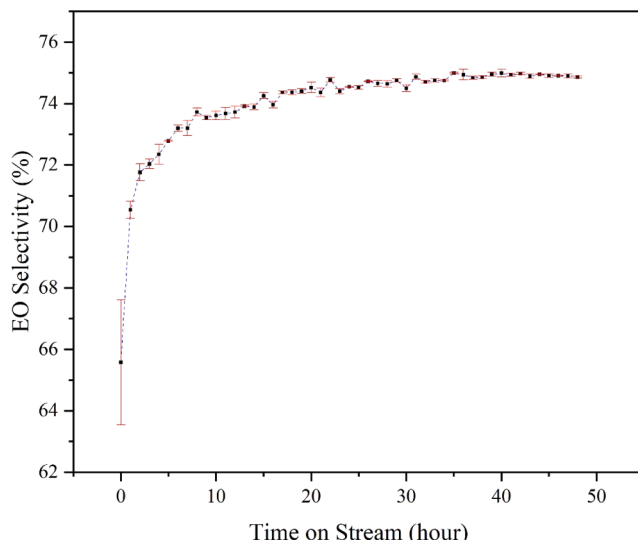


Fig. 13. EO selectivity of 5 wt% silver nanowire catalyst as a function of time on stream at a constant 10 % ethylene conversion.

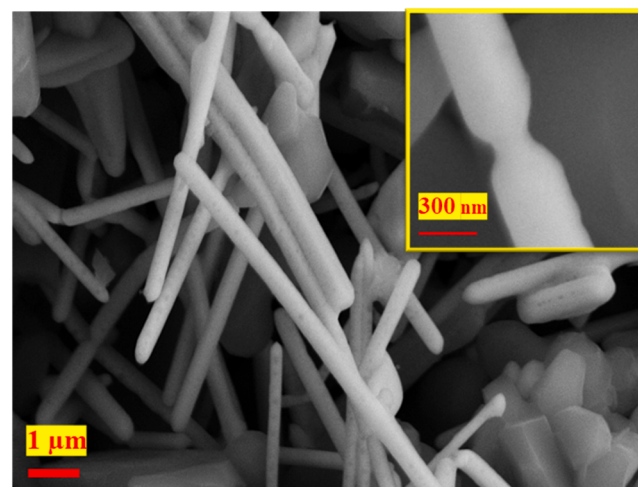


Fig. 14. SEM image of spent silver nanowires after 50 hours on stream. Inset: magnified view of the middle of a single silver nanowire, highlighting the necking phenomenon.

nanowires. In this process, nanowires featuring (100) facets undergo a transformation into spherical particles characterized by (111) facets, reflecting a lower energy state. The initiation of this phenomenon involves localized thinning at specific points along the nanowire diameter, eventually leading to the division of a single nanowire into two or more shorter counterparts. This transformative sequence persists until all nanowires undergo fragmentation, forming shorter nanowires and, subsequently, spherical particles. Importantly, the rate of nanowire sintering is contingent upon environmental and geometrical factors, including atmospheric conditions and temperature, as well as the initial thickness of the nanowire diameter [48].

In a distinct region where AgNWs are positioned on the support, notable changes are observed, as illustrated in Fig. 15. Tiny pores become apparent upon closer examination of specific nanowire edges at higher magnifications. These pores are attributed to the reaction conditions leading to atomic rearrangements, as documented in literature [49,50]. Ensuring consistency in observing morphological changes throughout the sample's lifespan is imperative. Thus, a broader depiction within Fig. 16 provides a view of AgNWs on the support. Examination of individual nanowires at this scale unveils similar pores along their edges, indicative of the active participation of these nanowires in the EPO reaction. Consequently, the SEM image of silver nanowires, captured at 10 μm scale, underscores the resilience of the majority of nanowires. This resilience is evident as they remain structurally intact even after prolonged exposure to the reaction environment for several days, without a discernible decline in their catalytic activity and selectivity.

Upon observing the rearrangement of silver atoms, it was crucial to investigate their possible effect on the catalyst's activity, selectivity and

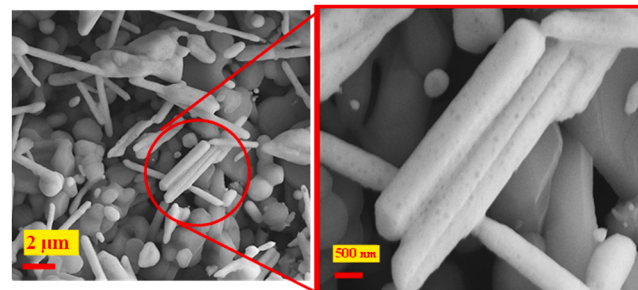


Fig. 15. SEM image of spent silver nanowires after 50 hours on stream, with a zoomed-in section highlighting the disarrangement of silver atoms.

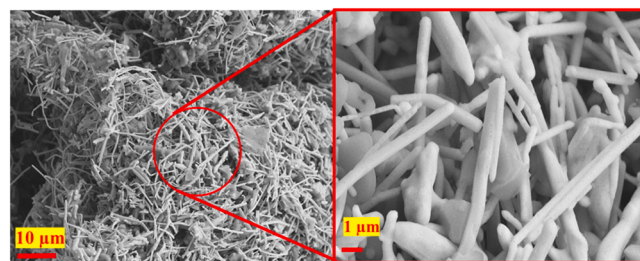


Fig. 16. SEM image of spent silver nanowires at a larger scale after 50 hours on stream, indicating intact morphology.

stability by conducting an experiment to examine the hysteresis effect. To address this, data were gathered after achieving stability in the results. The experimentation commenced with a 1:1 ratio of ethylene to oxygen and progressed through subsequent ratios of 1:3 and 1:5, followed by a reversal to 1:3 and 1:1, as depicted in Fig. 17, facilitating an assessment of reproducibility. The data points were recorded at hourly intervals, and each ratio was subjected to a runtime of approximately 12 hours. Notably, the results pertaining to the 1:1 and 1:3 ratios of ethylene to oxygen in the reverse sequence exhibited a remarkable concordance with their counterparts in the forward sequence. This concurrence strongly suggests that the observed silver atom rearrangement does not exert a discernible influence on the catalytic selectivity of the AgNWs, and no hysteresis effect was observed.

Confirming our previous observations from SEM images, the spent AgNWs displayed no signs of sintering even after several days on stream. A diameter distribution histogram for the spent supported silver nanowires is presented in Fig. 18. The average diameter calculated for the silver nanowires was 248 nm with a standard deviation of 70 nm, closely resembling that of the fresh catalysts. The slight difference may be attributed to measurement errors. Additionally, the thinnest silver nanowires, possibly with diameters below 100 nm, might have sintered during the reaction, as addressed in our previous study [27], and thus were not present in the spent catalyst in the same quantity as in the fresh catalyst. This could result in a slight larger average diameter for the spent AgNWs compared to the fresh ones. Sintering, a phenomenon not exclusive to silver nanowires or nanocubes, can also affect spherical particle catalysts due to Ostwald Ripening, especially pronounced in dynamic silver catalysts [12]. In the case of the silver spherical catalysts examined, with an average diameter of 786 nm and the largest diameter reaching 2 μm, noticeable sintering occurred, leading to larger spherical

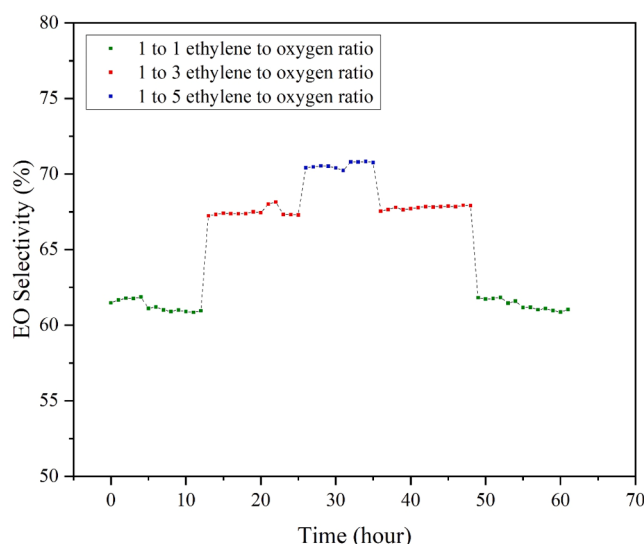


Fig. 17. Investigation of hysteresis effect on silver nanowires catalyst.

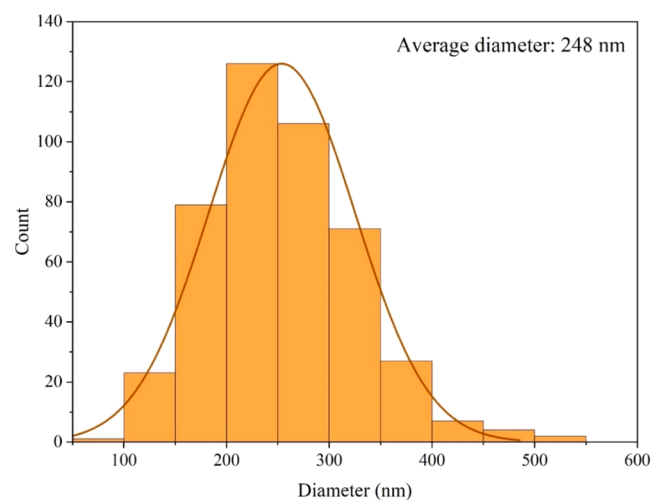


Fig. 18. Histogram of diameter distribution of spent silver nanowire catalysts after 50 hours on stream.

particles with diameters approaching 7–8 μm, as shown in Fig. 19.

5. Conclusion

In this study, we have not only demonstrated the significant impact of silver catalyst shapes on ethylene oxide (EO) selectivity, reflecting the diverse faceting of silver, but also advanced EO selectivity by promoting silver nanowires (AgNWs) with Cs, representing a novel exploration in this field. The scaling up of the modified polyol method was detailed to enhance the reproducibility of silver nanowires synthesis, followed by an explanation of the procedure for Cs promotion of the silver nanowires. Utilizing cesium acetate as the precursor, which decomposes at a lower temperature compared to the sintering temperature of silver nanowires, and employing ethanol as a crucial solvent for improved distribution of synthesized silver nanowires on the support, were highlighted. Cs loadings ranging from unpromoted to 66, 133, and 200 ppm were explored to determine the best loadings based on the EO selectivity of the promoted catalysts. Due to the size-dependent nature of the reaction on Ag nanoparticles, two different sizes of silver spherical particles were synthesized, with average diameters of 211 nm and 786 nm,

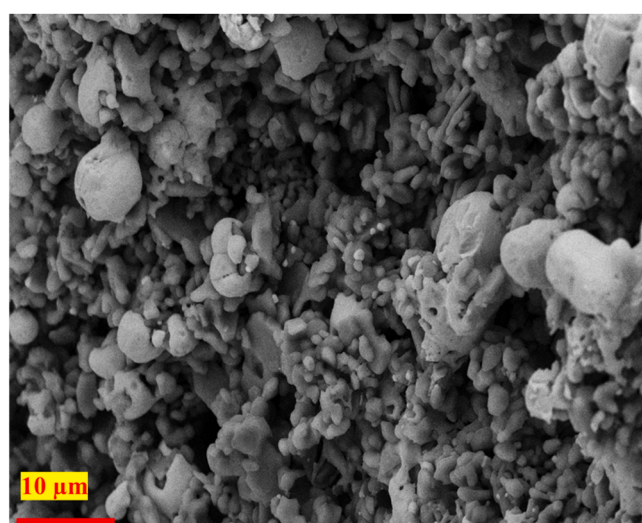


Fig. 19. SEM image of spent silver spherical catalyst (AgSPs_Sample 3) with an average initial diameter of 786 nm, showing evidence of silver particle sintering after reaction.

for comparison with silver nanowires. The synthesis of smaller spherical catalysts involved the use of ethylenediamine as a surfactant, resulting in enhanced interaction between the silver precursor and the support, leading to better distribution and smaller particle size. The diameter of the smaller silver spherical catalysts was set to be similar to that of the silver nanowires, ensuring comparable characteristic lengths. The effects of oxygen partial pressure on both unpromoted and promoted AgNWs were investigated across three different ethylene to oxygen ratios (1–1, 1–3, and 1–5), revealing increased EO production with rising oxygen partial pressure due to the positive reaction order with respect to oxygen for EO formation. Furthermore, unpromoted AgNWs exhibited significantly higher EO selectivity compared to even the promoted AgSPs, underscoring the superior selectivity of AgNWs and Ag(100) over AgSPs and Ag(111). At 66-ppm Cs promotion and 5 wt% silver loading, AgNWs achieved nearly 80 % EO selectivity at 10 % ethylene conversion, demonstrating the effectiveness of AgNWs catalysts in EO production. SEM images of spent AgNWs revealed that the catalyst maintained its morphology and EO selectivity even after prolonged exposure to the reaction stream, demonstrating exceptional stability. Unlike most literature studies, which do not investigate the stability of AgNWs beyond a few hours, our work extended the stability analysis for up to ten days. We thoroughly addressed the changes that occurred during the reaction, providing valuable insights into the long-term performance of AgNWs, which is often overlooked in previous research. Finally, comparison with literature results indicated that the Cs-promoted AgNWs investigated in this study exhibited EO selectivity comparable to that of promoted and Cl-added silver spherical catalysts reported in the literature, despite having half the silver loading.

CRediT authorship contribution statement

Lauterbach Jochen: Writing – review & editing, Supervision, Funding acquisition. **Shariati Kaveh:** Writing – review & editing, Writing – original draft, Methodology, Investigation, Formal analysis, Conceptualization. **Mehrani Azadeh:** Writing – review & editing, Formal analysis. **Corsello Trevor:** Formal analysis. **Kelley Mason:** Formal analysis.

Declaration of Competing Interest

The authors declare that they have no known competing financial interests or personal relationships that could have appeared to influence the work reported in this paper.

Acknowledgment

The authors express their gratitude to the Smart State Center of Economic Excellence for Strategic Approaches to the Generation of Electricity (SAGE) for funding this project, the University of South Carolina Electron Microscopy Center for providing access to instrumentation and offering scientific and technical guidance, the Saint-Gobain Company for generously supplying the SA5562 (α -Al₂O₃) support, and Chemix.org for providing a sketching website used for sketching the synthesis method diagram.

Appendix A. Supporting information

Supplementary data associated with this article can be found in the online version at [doi:10.1016/j.apcata.2025.120200](https://doi.org/10.1016/j.apcata.2025.120200).

Data availability

Data will be made available on request.

References

- [1] J.E. van den Reijen, et al., Preparation and particle size effects of Ag/ α -Al₂O₃ catalysts for ethylene epoxidation, *J. Catal.* 356 (2017) 65–74.
- [2] S. Wu, B.J. Tatarchuk, A.J. Adamczyk, Ethylene oxidation on unpromoted silver catalysts: reaction pathway and selectivity analysis using DFT calculations, *Surf. Sci.* 708 (2021) 121834.
- [3] S. Rebsdat, Ethylene oxide, *Encycl. Toxicol.* Third Ed. (2014) 535–538, <https://doi.org/10.1016/B978-0-12-386454-3.00021-X>.
- [4] Maximize Market Research. Ethylene Oxide Market: Global Industry Analysis and Forecast (2022–2029). <http://www.maximizemarketresearch.com/market-report/ethylene-oxide-market/41828/> (2023).
- [5] Théodore Ernie Lefort. Process for the production of ethylene oxide, US Patent US1998878A. (1931).
- [6] J.T. Jankowiak, M.A. Bartea, Ethylene epoxidation over silver and copper-silver bimetallic catalysts: I. Kinetics and selectivity, *J. Catal.* 236 (2005) 366–378.
- [7] M. Mavrikakis, D.J. Doren, M.A. Bartea, Density functional theory calculations for simple oxametallacycles, *Trends Across Period.* Table 5647 (1998) 394–399.
- [8] J.T. Jankowiak, M.A. Bartea, Ethylene epoxidation over silver and copper-silver bimetallic catalysts: II. Cs and Cl promotion, *J. Catal.* 236 (2005) 379–386.
- [9] M.O. Ozbek, I. Onal, R.A. Van Santen, Why silver is the unique catalyst for ethylene epoxidation, *J. Catal.* 284 (2011) 230–235.
- [10] M.O. Özbe, R.A. Van Santen, The mechanism of ethylene epoxidation catalysis, *Catal. Lett.* 143 (2013) 131–141.
- [11] K.C. Waugh, M. Hague, The detailed kinetics and mechanism of ethylene epoxidation on an oxidised Ag/ α -Al₂O₃ catalyst, *Catal. Today* 157 (2010) 44–48.
- [12] A.J.F. van Hoof, R.C.J. van der Poll, H. Friedrich, E.J.M. Hensen, Dynamics of silver particles during ethylene epoxidation, *Appl. Catal. B Environ.* 272 (2020) 118983.
- [13] T. Pu, H. Tian, M.E. Ford, S. Rangarajan, I.E. Wachs, Overview of selective oxidation of ethylene to ethylene oxide by Ag catalysts, *ACS Catal.* 9 (2019) 10727–10750.
- [14] M. Huš, A. Hellman, Dipole effect on ethylene epoxidation: influence of alkali metals and chlorine, *J. Catal.* 363 (2018) 18–25.
- [15] S. Linic, M.A. Bartea, On the mechanism of Cs promotion in ethylene epoxidation on Ag, *J. Am. Chem. Soc.* 126 (2004) 8086–8087.
- [16] D. Ren, H. Xu, J. Li, J. Li, D. Cheng, Origin of enhanced ethylene oxide selectivity by Cs-promoted silver catalyst, *Mol. Catal.* 441 (2017) 92–99.
- [17] M. Atkins, J. Couves, M. Hague, B.H. Sakakini, K.C. Waugh, On the role of Cs, Cl and subsurface O in promoting selectivity in Ag/ α -Al₂O₃ catalysed oxidation of ethene to ethene epoxide, *J. Catal.* 235 (2005) 103–113.
- [18] W. Diao, C.D. Digilio, M.T. Schaal, S. Ma, J.R. Monnier, An investigation on the role of Re as a promoter in Ag-Cs-Re/ α -Al₂O₃ high-selectivity, ethylene epoxidation catalysts, *J. Catal.* 322 (2015) 14–23.
- [19] Mingle, K.B. Combinatorial Study of Oxidation Catalysts: Uncovering Synthesis-Structure-Activity Relationships. (University of South Carolina, 2018).
- [20] M. Huš, A. Hellman, Ethylene epoxidation on Ag(100), Ag(110), and Ag(111): a joint Ab initio and kinetic Monte Carlo study and comparison with experiments, *ACS Catal.* 9 (2019) 1183–1196.
- [21] A.J.F. Van Hoof, E.A.R. Hermans, A.P. Van Bavel, H. Friedrich, E.J.M. Hensen, Structure sensitivity of silver-catalyzed ethylene epoxidation, *ACS Catal.* 9 (2019) 9829–9839.
- [22] P. Christopher, S. Linic, Shape- and size-specific chemistry of Ag nanostructures in catalytic ethylene epoxidation, *ChemCatChem* 2 (2010) 78–83.
- [23] Y.M. Chang, I. Lu, Te, C.Y. Chen, Y.C. Hsieh, P.W. Wu, High-yield water-based synthesis of truncated silver nanocubes, *J. Alloy. Compd.* 586 (2014) 507–511.
- [24] S.S. Sangaru, et al., Surface composition of silver nanocubes and their influence on morphological stabilization and catalytic performance in ethylene epoxidation, *ACS Appl. Mater. Interfaces* 7 (2015) 28568–28576.
- [25] P. Zhang, et al., Silver nanowires: synthesis technologies, growth mechanism and multifunctional applications, *Mater. Sci. Eng. B Solid-State Mater. Adv. Technol.* 223 (2017) 1–23.
- [26] W.M. Schuette, W.E. Buhro, Polyol synthesis of silver nanowires by heterogeneous nucleation; Mechanistic aspects influencing nanowire diameter and length, *Chem. Mater.* 26 (2014) 6410–6417.
- [27] K. Shariati, Shape-Selective Silver Catalysts for Ethylene Epoxidation, 2021.
- [28] Shariati, K. Shape-Selective Silver Catalysts for Ethylene Epoxidation. (University of South Carolina, 2021).
- [29] Y. Sun, B. Gates, B. Mayers, Y. Xia, Crystalline silver nanowires by soft solution processing, *Nano Lett.* 2 (2002) 165–168.
- [30] Y. Sun, B. Mayers, T. Herricks, Y. Xia, Polyol synthesis of uniform silver nanowires: a plausible growth mechanism and the supporting evidence, *Nano Lett.* 3 (2003) 955–960.
- [31] L. Cao, et al., Rapid and facile synthesis of high-performance silver nanowires by a halide-mediated, modified polyol method for transparent conductive films, *Nanomaterials* 10 (2020).
- [32] Y. Gao, et al., Evidence for the monolayer assembly of poly(vinylpyrrolidone) on the surfaces of silver nanowires, *J. Phys. Chem. B* 108 (2004) 12877–12881.
- [33] H.I. Sang, T.L. Yun, B. Wiley, Y. Xia, Large-scale synthesis of silver nanocubes: the role of HCl in promoting cube perfection and monodispersity, *Angew. Chem. - Int. Ed.* 44 (2005) 2154–2157.
- [34] R.J. Chimentao, et al., Effects of morphology and cesium promotion over silver nanoparticles catalysts in the styrene epoxidation, *J. Mater. Sci.* 42 (2007) 3307–3314.

- [35] M.M. Rahman, B.T. Egelske, K. Enyekwe, J.M. Tengco, J.R. Monnier, Characterization of Ag/ α -Al₂O₃ olefin epoxidation catalysts containing promoters and co-promoters using pulse hydrogen titration methods, *J. Catal.* 429 (2024).
- [36] Y. Sun, Y. Xia, Shape-controlled synthesis of gold and silver nanoparticles, *ChemInform* 34 (2003) 2176–2180.
- [37] B. Wiley, Y. Sun, B. Mayers, Y. Xia, Shape-controlled synthesis of metal nanostructures: the case of silver, *Chem. - A Eur. J.* 11 (2005) 454–463.
- [38] K. McCullough, T. Williams, K. Mingle, P. Jamshidi, J. Lauterbach, High-throughput experimentation meets artificial intelligence: a new pathway to catalyst discovery, *Phys. Chem. Chem. Phys.* 22 (2020) 11174–11196.
- [39] J. Dellamorte, M.A. Bartea, J. Lauterbach, Investigation of Ag Based Catalysts for Ethylene Epoxidation: High Throughput Studies and Characterization. (University of Delaware, 2009).
- [40] B.T. Egelske, W. Xiong, H. Zhou, J.R. Monnier, Effects of the method of active site characterization for determining structure-sensitivity in Ag-catalyzed ethylene epoxidation, *J. Catal.* 410 (2022) 221–235.
- [41] B.W.J. Chen, B. Wang, M.B. Sullivan, A. Borgna, J. Zhang, Unraveling the synergistic effect of Re and Cs promoters on ethylene epoxidation over silver catalysts with machine learning-accelerated first-principles simulations, *ACS Catal.* 12 (2022) 2540–2551.
- [42] C.J. Chen, J.W. Harris, A. Bhan, Kinetics of ethylene epoxidation on a promoted Ag/ α -Al₂O₃ catalyst—the effects of product and chloride Co-feeds on rates and selectivity, *Chem. - A Eur. J.* 24 (2018) 12405–12415.
- [43] K.R. Iyer, A. Bhan, Particle size dependence of ethylene epoxidation rates on Ag/ α -Al₂O₃ catalysts: why particle size distributions matter, *J. Catal.* 420 (2023) 99–109.
- [44] H. Mao, J. Feng, X. Ma, C. Wu, X. Zhao, One-dimensional silver nanowires synthesized by self-seeding polyol process, *J. Nanopart. Res.* 14 (2012).
- [45] R.J. Chimentão, et al., Styrene epoxidation over cesium promoted silver nanowires catalysts, *J. Mol. Catal. A Chem.* 258 (2006) 346–354.
- [46] A. Chongterdtoonskul, J.W. Schwank, S. Chavadej, Effects of oxide supports on ethylene epoxidation activity over Ag-based catalysts, *J. Mol. Catal. A Chem.* 358 (2012) 58–66.
- [47] P.H. Keijzer, J.E. van den Reijen, C.J. Keijzer, K.P. de Jong, P.E. de Jongh, Influence of atmosphere, interparticle distance and support on the stability of silver on α -alumina for ethylene epoxidation, *J. Catal.* 405 (2022) 534–544.
- [48] M. Rauber, F. Muench, M.E. Toimil-Molares, W. Ensinger, Thermal stability of electrodeposited platinum nanowires and morphological transformations at elevated temperatures, *Nanotechnology* 23 (2012).
- [49] Y. Ma, et al., Tailoring of the proximity of platinum single atoms on CeO₂ using phosphorus boosts the hydrogenation activity, *ACS Catal.* 9 (2019) 8404–8412.
- [50] X. Ye, et al., Insight of the stability and activity of platinum single atoms on ceria, *Nano Res* 12 (2019) 1401–1409.